



HIGH SENSITIVITY OF La_2O_3 doped CdS FOR BLUE REGION DETECTOR

Ali A. Safi & Isam M. Ibrahim

Department of Physics, College of Science, University of Baghdad

ABSTRACT

Cadmium Sulfide (CdS) has different applications in optoelectronic devices like solar cells, photodetectors *etc.* In the present work pure CdS and La_2O_3 doped CdS at different ratio were deposited on glass and silicon substrates by using Chemical Spray Pyrolysis Method. The structural, optical and surface morphologies of CdS thin films have been investigated. It is found that the effect of La doped CdS enhancement the film crystallinity, reduce grain boundaries, increase in (transmittance and PL) intensity. Low noise, high quantum efficiency, and sensitivity reach to 2000%.

KEYWORDS: Detectors, rare earth elements, high sensitivity.

INTRODUCTION

In the last decades, there has been a fast increase in research on nanostructures. A variety of structures, such as surface passivity particles, clusters and multilayers of different materials have been manufactured and characterized. By using different techniques, the scaling behavior of the properties with size was studied in these investigations. In semiconductors, it was confirmed that as the radius of the crystallite come close to the Bohr radius of an exaction, the energy gap begins to widen, this is due to the quantum size effect^[1]. One of an important application of semiconductor materials, optoelectronic circuits. Many semiconductor materials have been used for the production of photo detectors. And the large range of band gaps of these materials leads to a wide spectral response ranging from far-infrared to ultraviolet (UV) light^[2]. While conventional photo detectors are usually in the film or bulk configurations, the unique and significant properties of nanomaterials. Among the compound semiconductors, CdS is the most promising material for detecting visible radiation due to its high sensitivity and primary band gap of 2.42 eV (516nm) for bulk, while 2nm size nanoparticles have 3.57 eV band gap^[3]. In particular, CdS has been extensively studied because of its large value of band gap (E_g), which allows light emission between blue and red wavelengths, due to the large band gap of CdS nanoparticles, it is used as window material in hetero junction solar cells^[4]. CdS has three types of crystal structures namely hexagonal wurtzite, cubic zinc blend and high pressure rock-salt phase. Among these the hexagonal wurtzite has been intensively investigated because it is the most stable of the three phases and can be easily synthesized. Hexagonal phase has been observed in both the bulk and nanocrystalline CdS while cubic and rock-salt phases are observed only in nanocrystalline CdS^[5]. Rare earth-doped CdS, are very promising material as its band gap relate closely to the visible part of the spectrum. In addition, band-to-band transitions occurring in this material make it suitable for applications in many electro-optical devices^[6]. The rare earth ions possess

fascinating optical properties. Such as lanthanum (La), which no much work was reported regarding effect of the (La). Bhushan *et al.*^[7] reported that PL in La doped (Cd-Pb) S thin films showed emission in green region with peak at 530nm under 365nm excitation. To further investigate and establish the role of La in the host nanocrystalline CdS semiconductor, La was selected as impurity for nanocrystalline studies. For a good photoconductive device, requires efficient transport of charge carriers to electrode and efficient charge separation^[8]. It is well known that the recombination centers, which lying in the forbidden energy zone or the trapping states control the rise and decay curves of photocurrent^[9].

II. Experimental work

Cadmium chloride ($\text{CdCl}_2 \cdot \text{H}_2\text{O}$) from THOMAS BAKER Company, of molecular weight (201.33 g/mol) and purity 99.9%, which is a fast-soluble white crystal in distilled water and ethanol as a source of cadmium ion and use thiourea ($\text{NH}_2 \cdot \text{SC} \cdot \text{NH}_2$) from Thomas Baker Company, of molecular weight (76.12 g/mol) and purity 99.9%, as a source of sulphur ion. Were both separately dissolved in 50 ml of distilled water and 10 ml ethanol and then mixed the Cadmium chloride solution with Thiourea using a magnetic stirrer with temperature 30°C for 30 minutes to complete the solubility process and obtain a pure CdS solution. The solution was present at a molecular concentration (0.2M). While La_2O_3 dissolved in 40 ml of distilled water and 10 ml ethanol using a magnetic stirrer with temperature 30°C for 30 minutes, The solution was present at a molecular concentration (0.2M) and add (5, 10 and 15) ml from Lanthanum Oxide deposition to (45, 40 and 35) ml of Cd deposition and put this mixed on the magnetic stirrer with 30°C for 30 minute. And the mixture add to 50ml of sulfide in same steps above to get CdS: La solution with concentration of doping 10, 20 and 30%. Glass and silicon substrates of dimensions (2.5×1) cm and (1×1) cm respectively cleaned with distilled water, ethanol and ultrasonic cleaner, silicon substrate of area 1cm² cleaned in mixed solution of 9ml distilled water and 1ml of ethanol, after that use air flow at room temperature to

drying these substrate. The deposition spray on substrate by Chemical Spray Pyrolysis Method with temperature 200°C and the distance was set as 20cm between the nozzle and substrates, the growth of samples by rate 0.6 ml/min, This means that it takes about two and a half hours to spray the solution. Aluminum electrodes were used on the surface of CdS pure and CdS: La thin films . The structure of deposited thin film has been analysis using X-Ray diffraction system type MiniFlex II, An optical spectroscopic reflectometer used to measured of thin film thickness, surface morphology used FEI Nova nanoSEM 450 (The Netherlands) Field Emission Scanning Electron Microscope (FESEM), optical properties (T, and E_g) were studied by Spectrophotometer (UV / 1800 / Shimadzu) of Japan, photoluminescence of thin films were measured by RF-551 Spectrofluorometric Detector (Shimadzu), photoconductivity and photosensitivity were studied by sensitive digital electrometer type Keithly (2400).

RESULTS & DISCUSSION

1. X-Ray Diffraction Analysis

Fig. (1) shows the X-ray diffraction pattern of the undoped CdS and doped CdS: La thin film at ratio (10, 20 and 30%). All patterns In this figure noted that the pure CdS shows the film exhibited hexagonal (wurtzite) crystal structure as indicated by the absence of characteristic (200) and (311) peaks of the cubic CdS structure, where the XRD peaks can be attributed to (100), (002), (101), (102), (110), (103) and (112) of hexagonal CdS corresponding to JCPDS File (No. 96-101-1055), with a preferential orientation along the (002) plane. The average crystallite size is calculated from Scherer formula [10]:

$$D = 0.9 / (\cos \theta) \dots \dots \dots (1)$$

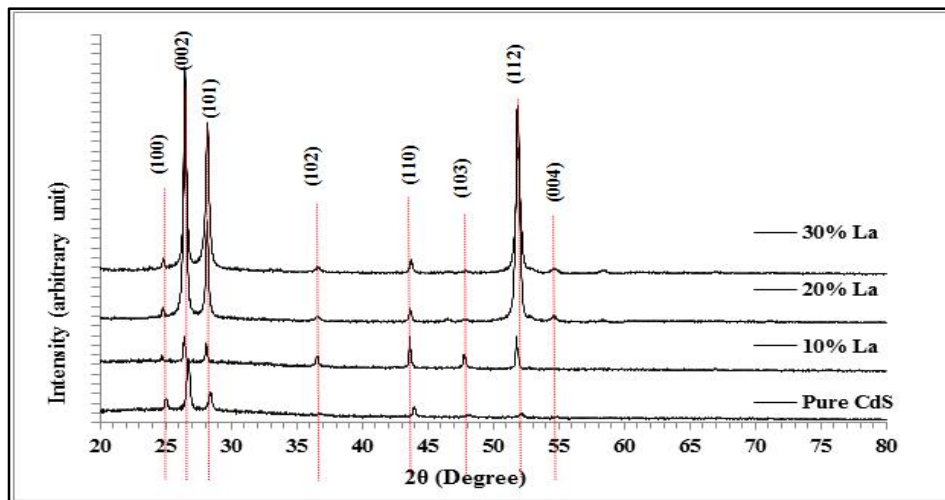


FIGURE 1: shows the XRD patterns of pure CdS and CdS: La at 10, 20 and 30%

TABLE 1: Structural parameters for pure CdS and CdS:La at 10,20 and 30%

Sample	2θ (Deg.)	FWHM (Deg.)	d _{hkl} Exp.(Å)	G.S (nm)	d _{hkl} Std.(Å)	Phase	hkl
Pure	25.0525	0.1690	3.5516	48.2	3.5940	Hex. CdS	(100)
	26.7571	0.2010	3.3291	40.6	3.3685	Hex. CdS	(002)
	28.4310	0.2457	3.1368	33.4	3.1710	Hex. CdS	(101)
	52.1577	0.3072	1.7522	28.8	1.7667	Hex. CdS	(112)
10% La	24.7241	0.2207	3.5980	36.9	3.5940	Hex. CdS	(100)
	26.4459	0.2208	3.3676	37.0	3.3685	Hex. CdS	(002)
	28.1236	0.2208	3.1704	37.1	3.1710	Hex. CdS	(101)
	51.7881	0.2649	1.7639	33.3	1.7667	Hex. CdS	(112)
20% La	24.7682	0.2207	3.5917	36.9	3.5940	Hex. CdS	(100)
	26.4901	0.3532	3.3620	23.1	3.3685	Hex. CdS	(002)
	28.1678	0.2207	3.1655	37.1	3.1710	Hex. CdS	(101)
	51.8764	0.4415	1.7611	20.0	1.7667	Hex. CdS	(112)
30% La	24.8124	0.2207	3.5854	36.9	3.5940	Hex. CdS	(100)
	26.5342	0.3091	3.3566	26.4	3.3685	Hex. CdS	(002)
	28.2119	0.3532	3.1606	23.2	3.1710	Hex. CdS	(101)
	51.9205	0.3532	1.7597	25.0	1.7667	Hex. CdS	(112)

The average crystallite size of pure CdS is 40.6 nm, While for CdS doped with La at 10,20 and 30 % the particle size decreases to 26.04nm at (002) peak, this figure also reveal the decreasing in diffraction peaks intensities for

CdS:La10% for (100), (002) and (101), while observed increasing in diffraction peaks intensities for (102), (110), (103) and (112), and have preferential orientation along the (112) plane of hexagonal phase and there are no such

for impurity, which is the evidence of successful dissolution of La atoms in host structure. The decreasing and increasing in peaks intensities compare with those of pure CdS refer to the more random preferred orientation takes place and reduce particle size^[11]. The third and fourth patterns for doping ratio 20 and 30% respectively, observed an increasing in diffraction intensities and appear peak (004), with hexagonal phase and the preferential orientation along the peak (002), all X-ray data and grain size have been calculated for peaks (100, 002, 101 and 112) and listed in table (1).

Figure (2) (a-d) explain the images of FESEM of pure CdS and doped CdS:La at 10,20 and 30%, the magnification power is 50.0 kx, image (a) shows non homogeneous grains shapes and their size too, the surface is covered by

big grains with a triangular shape and other were small grains with undefined shape, the sample is composed of smooth and continuous morphology without having any pinholes, while image (b) reveal the changes in the grains shapes are triangles and a small amount of polygon shaped grains also appears through the surface, it is observed that the sizes of the grains are bigger than the grains in image (a), that consequences to assemble small grains to form big grain, it seems that the surface has less roughness and that agreement with S. Yılmaz *et al.*^[11]. Large proportion of the surface is covered by grains with worm-like shape and a smaller proportion in the form of triangles with big and small sizes in image (c), while in images (d) shapes like fig leaf with different size.

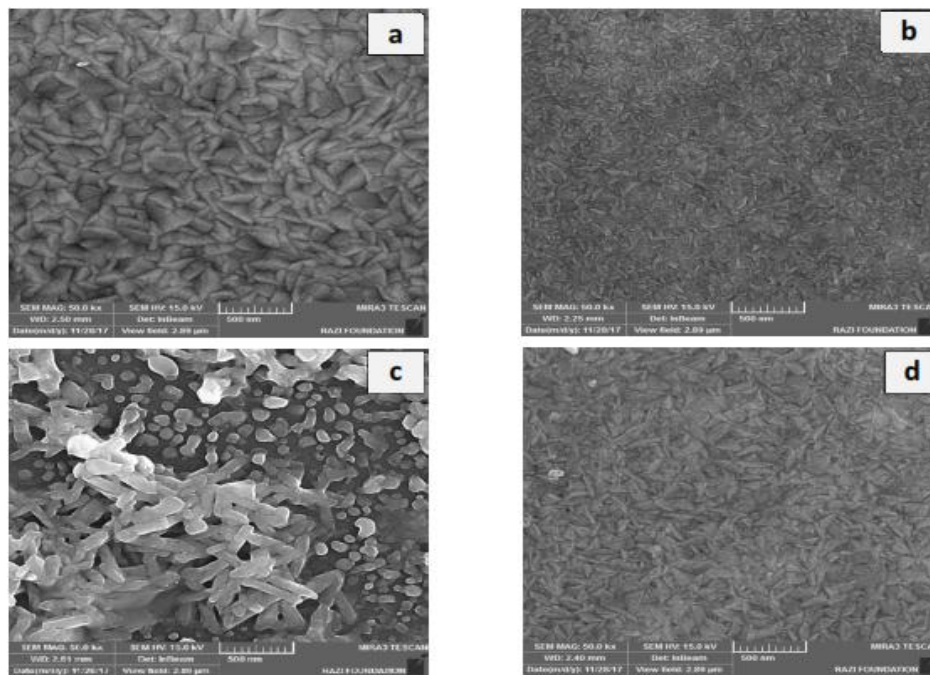


FIGURE 2. FESEM images (a) pure CdS (b) CdS:La at 10% (c) CdS:La at 20% (d) CdS:La at 30%

The transmittance and Optical properties

Figure (3), shows the transmittance spectra of pure CdS, and CdS:La at different ratio. Undoped CdS has transmittance of 60 % at the wavelength range of 516-1100 nm which is low due to the small grains with more grain boundaries (as mention in Figure. 2(a)) with respect to CdS:La ones, giving rise to an increase in the light

scattering from grain boundaries^[12,13]. While CdS: La at 10, 20 and 30% the transmittance values increases to 83, 85 & 89% respectively. The enhancement in transmittance value after doped La may be ascribed to the grain growth, leading to less grain boundaries and hence less light scattering from the grain boundaries^[14].

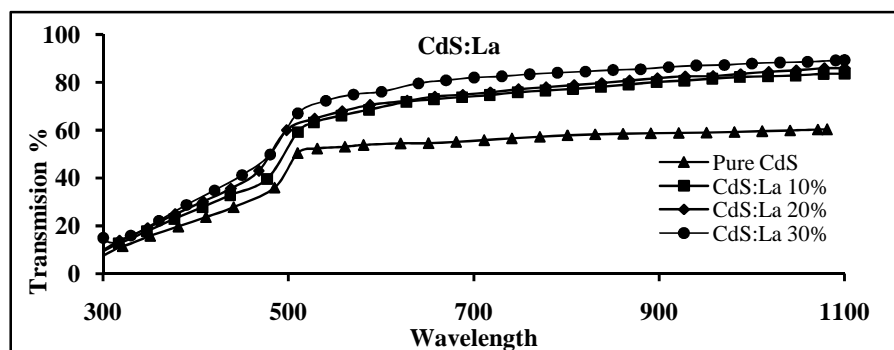


FIGURE 3. Transmittance for pure CdS and CdS:La thin films at different ratio

The optical energy gap of pure CdS and doped CdS:La, have been determined by using the Tauc plot analysis^[15], as shown in Fig (4), the optical energy gap of undoped CdS is ($E_g^{opt} = 2.57$ eV). While CdS:La at 10, 20 and 30%

are ($E_g^{opt} = 2.60, 2.68$ and 2.70 eV), that mean with dopant the optical energy band increase, which may be ascribed to the quantum confinement effect, this results are agreement with L. Saravanan *et al.*^[16].

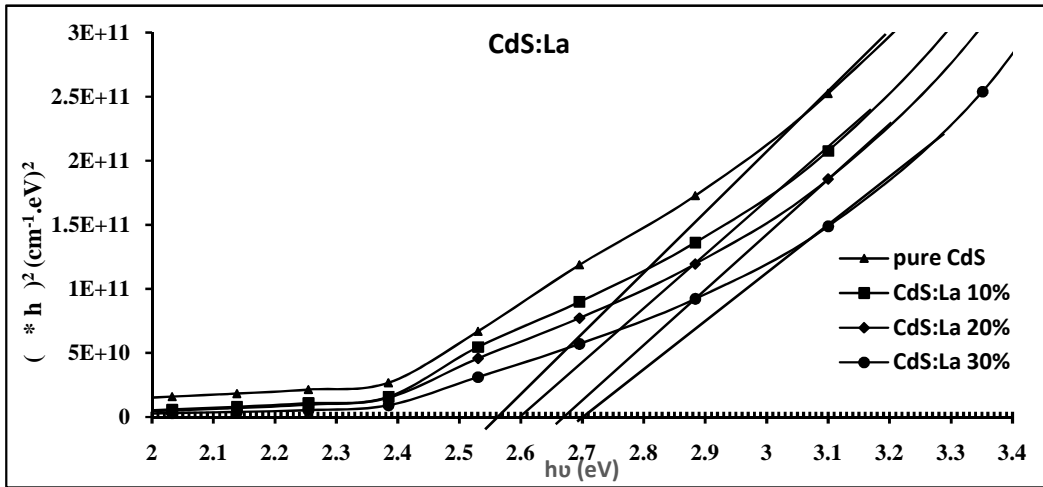


FIGURE 4: the optical energy gap for pure CdS, and CdS:La at different ratio

In Fig (5) shows the photoluminescence (PL) spectrum, where the excited wavelength is at 400 nm for pure CdS and CdS:La at 10, 20 and 30% thin films. For pure CdS there is a broad defect emission because the present of point defects such as cadmium vacancies (V_{Cd}), sulfur vacancies (V_s), cadmium interstitials I_{Cd} and sulphur interstitials (I_s), which act as luminescent centers. It is observed that three peaks, a broad peak centered at 430, the second peak centered at 530, and the third peak centered at 610nm, with UV, green and orange emission respectively. The UV emission attributed to transitions from the deep and shallow states^[17], the green emission band of the second

peak is due to electronic transition from conduction band to an acceptor level due to interstitial sulphur ions (I_s)^[18]. The origin of orange band is originating from the transition from the donor levels, created by the occupation interstitial sites of Cd atoms (I_{Cd}), to the valence band^[19]. For CdS:La at different ratio also observed same peaks with increasing of intensities as adding of La, this supports that these emissions are not due to direct transitions in energy bands of La^[20]. The improvement of the intensities in existence of La may due to the transitions between the excitonic levels of CdS and the energy levels due to La doped^[21].

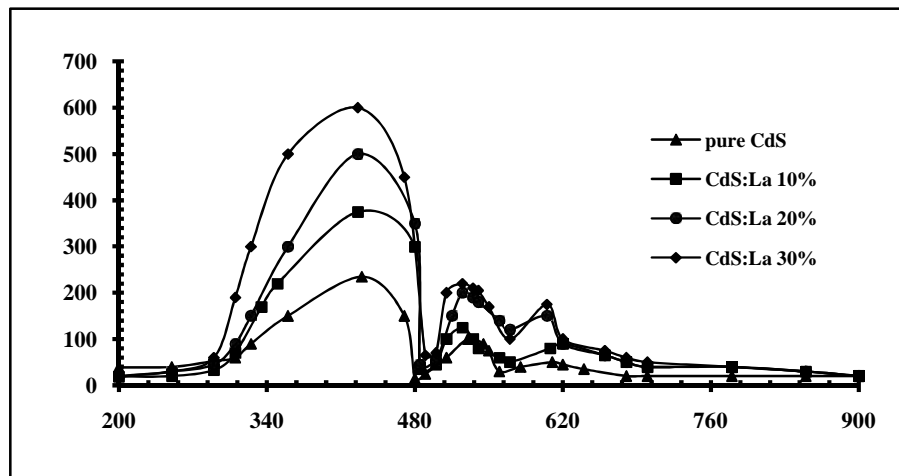


FIGURE 5: PL spectra of undoped CdS and CdS:La at different ratio

Figure of merit of photodetector

Figure (6) shows the Responsivity spectra $R(\lambda)$ for pure and La doped CdS photodetector, as shown in this figure the higher responsivity at wavelength (460, 550 and

680nm), the maximum increase in responsivity with La doping at 10% compare with pure CdS and CdS:La 20 and 30%, which may be due to triangles shape of the grains in CdS:La 10% thin film, which appear in figure 2 (b) .

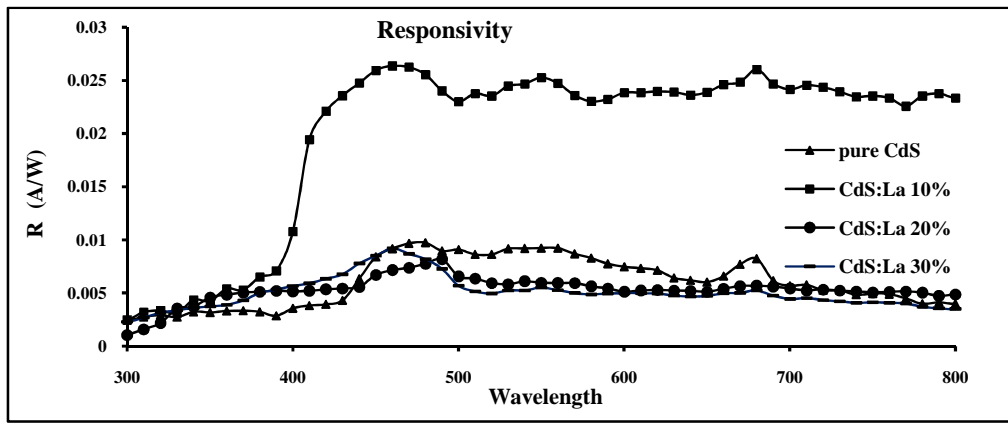


FIGURE 6. Responsivity spectra for pure CdS and CdS:La at different ratio

The quantum efficiency (η) for photoconductor device is consider a very important parameter, which by it can be recognized the optoelectronic effect, and it related to the

change of spectral responsively, as shown in Fig (7) for pure CdS and La doped CdS, the maximum value for quantum efficiency (η) is 7.1% at CdS: La 10%.

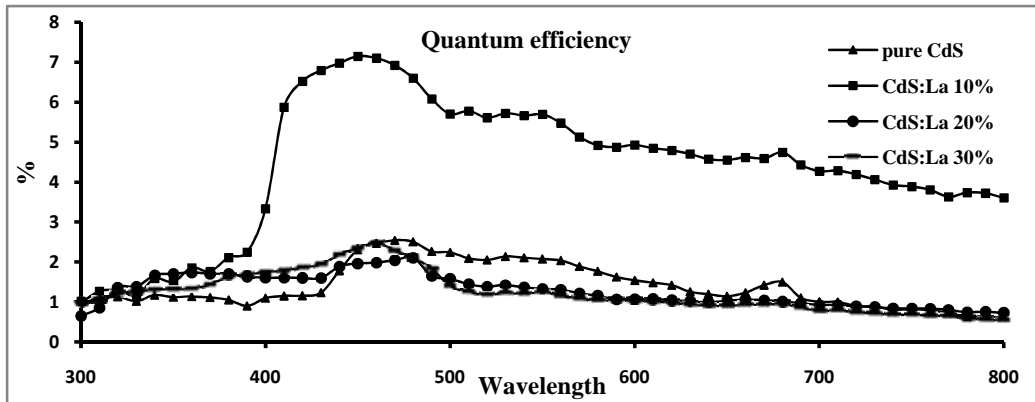


FIGURE 7. The Quantum Efficiency for pure CdS and CdS:La at different ratio

The noise in detector can be quantify by used the Noise Equivalent Power (NEP). Figure (8) shows the variation of NEP for pure CdS and CdS:La (10, 20 and 30%). It can be

observed that when the maximum of R occurs, in front of the minimum of NEP. It found that the lowest value of NEP was $(1.6 \times 10^{-12} \text{ W})$ at 460nm for CdS:La at 10%.

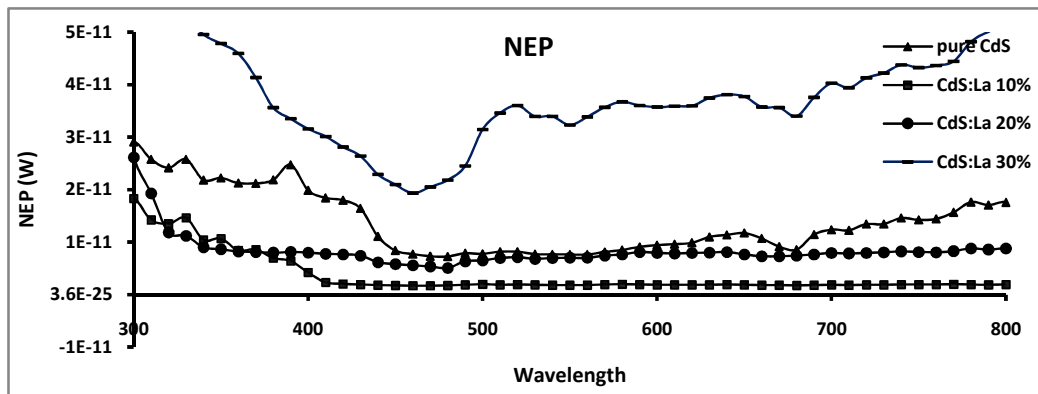


FIGURE 8. The NEP for pure CdS and CdS:La at different ratio

The detectivity (D) and the specific Detectivity (D^*) of pure CdS and doped CdS photodetector, can be calculated by take the reciprocal of the NEP and the reciprocal of the NEP normalized to the detector area of 0.1485 cm^2 and the band width of electrical noise f of (0.4427 Hz) . As

shown in figure (9) for pure CdS and CdS:La at (10, 20 and 30%). The D and D^* maximum values for CdS:La at 10% which equal to $(5.8 \times 10^{11} \text{ W}^{-1} - 1.4 \times 10^{11} \text{ jones})$ at 460nm, compare with the value for pure CdS $(1.2 \times 10^{11} \text{ W}^{-1} - 3.3 \times 10^{10} \text{ jones})$ at 460nm.

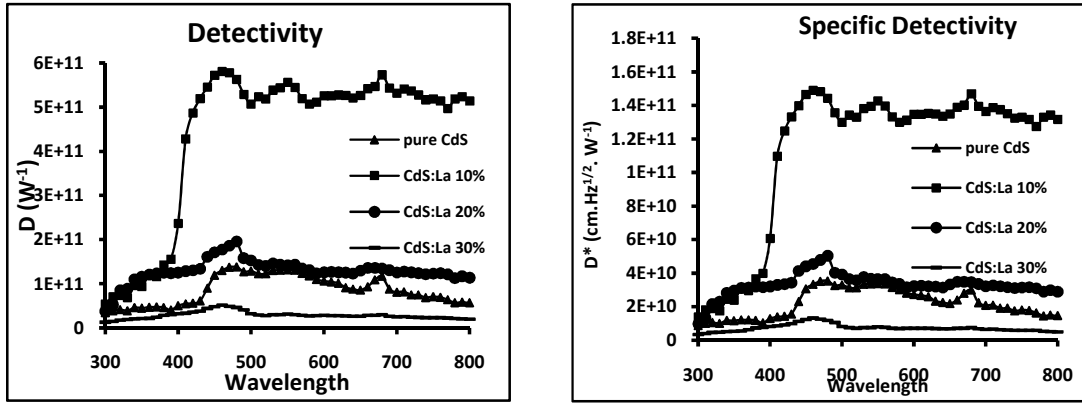


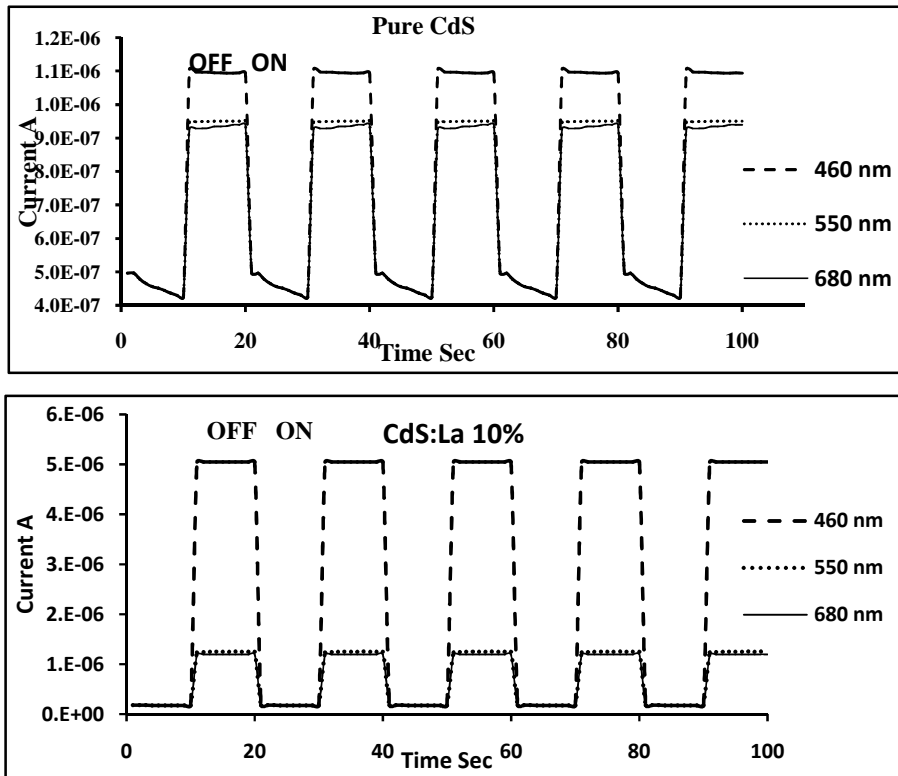
FIGURE 11. The Detectivity and specific Detectivity for pure CdS and CdS:La at different ratio

Photosensitivity properties of pure CdS and CdS:La at (10, 20 and 30%) photodetector has been studied, as shown in Fig 11, the plot of current with time. When the incident light with suitable wavelength was turned on, the photoconductivity increased and after light turned off, the current returned to its original value *i.e.*, the photo resistivity in decrease dark and increase in light. Pure CdS and CdS:La at 10% irradiative with wavelengths (460, 550 and 680nm), it is noted for pure CdS there is a good response speed to the incident light and that speed increase with La doping at 10%, this may be due to the unique characteristics of CdS:La nanoparticles, which are held to contribute to the significantly enhanced response speed as compared to CdS, this characteristics can be listed as (1) The higher crystal quality of CdS:La nanoparticles.

Because of reduce of defects, therefore, the photocurrent reaches a steady state rapidly in both the rise and decay stages (2) The high surface-to-volume ratio of CdS:La nanoparticles, the defects on the surface may act as recombination centers, which enhance the recombination of free carriers and shorten the decay time (3) The reduction of the recombination barrier in nanoparticles [22]. Sensitivity of the pure CdS and CdS:La at 10% thin films determined by [23]:

$$\text{Sensitivity (\%)} = (R_d - R_i) / R_i \text{ ----- (2)}$$

Where R_d is the Dark Resistance and R_i is the Light illuminated Resistance, and the data recorded in table 2.



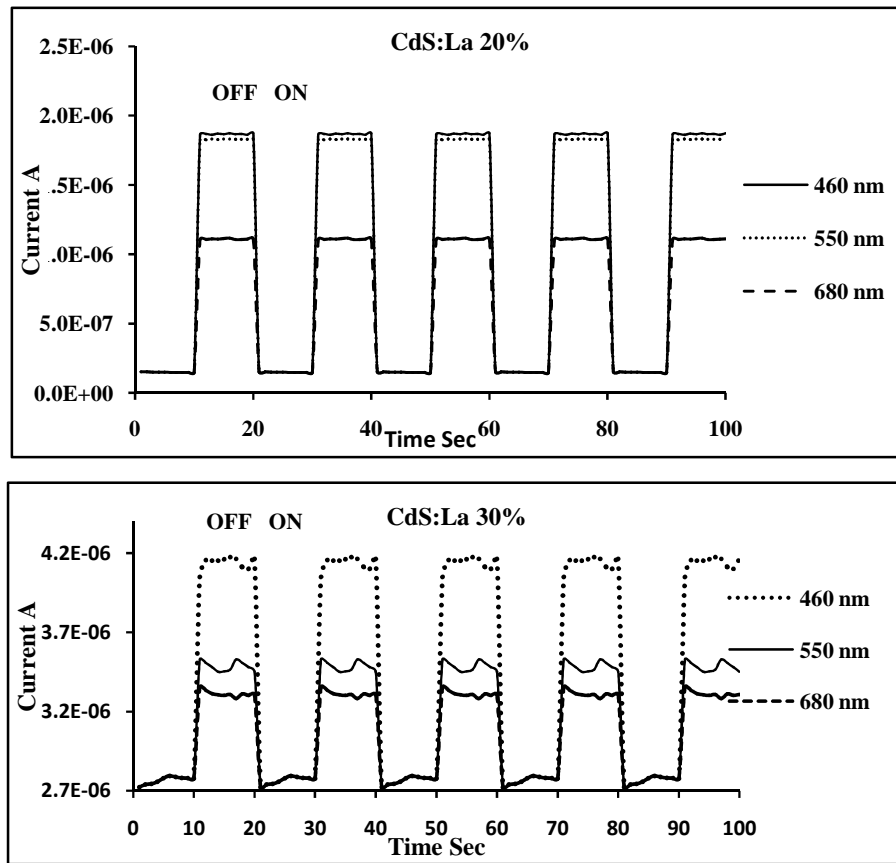


FIGURE 11. Time response of pure CdS and CdS:La at 10, 20 and 30%

TABLE 2. The sensitivity for pure CdS and CdS:La at 10, 20 and 30% corresponding to excitation wavelength

Thin film	nm	S%	nm	S%	nm	S%
Pure CdS	460	560	550	325	680	163
CdS:La 10%	460	2000	550	600	680	579
CdS:La 20%	460	1065	550	1034	680	650
CdS:La 30%	460	41	550	24	680	20

CONCLUSION

It has been successfully; synthesis lanthanum doped The Cadmium Sulfide (CdS) thin films at ratio 10, 20 and 30% were spray on substrate by Chemical Spray Pyrolysis Method with temperature 200°C. From the UV-Visible analysis the CdS:La thin films were having good transmission properties and from the Tauc's plot the band gap values are determined. The X-ray diffraction (XRD)-Analysis shows deposited thin films are in crystalline nature and the average crystallite size of the pure CdS and CdS:La thin films measured are (40.6–33.3nm). Photoluminescence of CdS and CdS:La thin films are tested and enhancement in PL intensity observed in presence of La. The sensitivity increases more than 200 times with addition of Lanthanum.

REFERENCES

- [1]. Efros, A. and Efros, A. Sov. "Phys.–Semiconductor". 1982, 16 772.
- [2]. Blank, T.V., Gol'dberg, Yu. A. "Semiconductors" 2003, 37 999.
- [3]. Banerjee, R., Jayakrishnan, R., Ayyub, P. (2000) "Effect of the size induced structural transformation on the band gap in CdS nanoparticles". J Phys Condens Matter, 12, 10647–54.
- [4]. Romeo, N., Bosio, A., Canevari, V., Podesta, A. (2004) Recent progress on CdTe/CdS thin film solar cells. Sol Energy", 77, 795–801.
- [5]. Ricolleau, C., Audinet, L., Gandais, M., Gacoin, T. "Structural transformations in II–VI semiconductor nanocrystals". Eur Phys J D 1999, 9, 565–70.
- [6]. Hang Li (2013) "Structural and Optoelectronic Properties of Rare Earth Doped Silicon Photonic Materials" Ph.D. Thesis. 2013.
- [7]. Bhushan, S., Mukherjee, M. and Bose, P., Mat. J. Sc. (Mat. In Electronics), 2002, 13 581.
- [8]. Tadaihiro Murakata, Kouske Aita, LiuHu.i Iha, Higuchi Takeshi Sato Shimio," Photoconductivity of n-type semiconductor nanoparticle-Doped poly (Nvinylcarba-zole", Mater Sci., 2007, 42 6279.
- [9]. Srivastava, S., Mishra, S.K., Yadav, R.S., Srivastava, R.K., Panday, A.C., Prakash, S.G. (2010) Photoconductivity and Darkconducti-Vity

- Studies of Mn-DOPED ZnS Nanoparticles", Digest Journal of Nanomaterials and Biostructures, 2010, 5 1,161–167.
- [10]. Cullity, B.D., Stock, S.R. (2001) "Elementary of X-ray Diffraction", Englewood Cliffs, 3rd ed., Prentice-Hall, New Jersey, 167- 171.
- [11]. Yilmaza, S., Törelib, S.B., Polatc, ., Olgard, M.A., Tomakine, M., Bacaksızd, E. (2017) "Enhancement in the optical and electrical properties of CdS thin Films through Ga and K co-doping.
- [12]. Guillen-Santiago, A., M. de la L. Olvera, A. Maldonado, R. Asomoza, Acosta, D.R. (2004) Electrical, structural and morphological properties of chemically sprayed F-doped ZnO films: effect of the ageing-time of the starting solution, solvent and substrate temperature", Phys. Stat. Sol. A 201 952-959.
- [13]. Kucukomeroglu, T., Bacaksiz, E., Terzioglu, C. Varilci, A. (2008) Influence of fluorine doping on structural, electrical and optical properties of spray pyrolysis ZnS films", Thin Solid Films, 516, 2913-2916
- [14]. Salih Yilmaz (2015) The investigation of spray pyrolysis grown CdS thin films doped With flourine atoms" Applied Surface Science.
- [15]. Badera, N., Godbole, B., Srivastava, S.B. Vishwakarma, P.N., Sharath Chandra, L.S., Jain, D., Gangrade, M., Shripathi, T., Sathe, V.G., "Ganesan, V. Quenching of photoconductivity in Fe doped CdS thin films prepared by spray pyrolysis technique", Appl. Surf. Sci. 254 (2008) 7042-7048.
- [16]. Saravanan, L., Pandurangan, A., Jayavel, R. (2012) Synthesis and luminescence enhancement of Cerium doped CdS Nanoparticles" 66 (2012) 343–345.
- [17]. Kumar, R., Das, R., Gupta, M., Ganesan, V. (2013) Compositional effect of antimony on structural, optical, and photoluminescence properties of chemically deposited (Cd1–xSbx) S thin films", Super lattices Microstruct. 2013,59 29-37.
- [18]. Sivaraman, T., Balu, A.R., Nagarethinam, V.S. (2014) Effect of magnesium incorporation on the structural, morphological, optical and electrical properties of CdS thin films", Mater. Sci. Semicond, Process, 27 915-923.
- [19]. Podesta, A., Armani, N., Salviati, G., Romeo, N., Bosio, A., Prato, M. (2006) "Influence of the fluorine doping on the optical properties of CdS thin films for photovoltaic applications" , Thin Solid Films 511-512 448-452.
- [20]. Smriti Agrawal, Ayush Khare (2011) Effect of La on optical and structural properties of CdS–Se films" Arabian Journal of Chemistry, 8: 450–455.
- [21]. Saravanan, L., Jayavel, R., Pandurangan, A., Liu, Jih-Hsin, Miao Hsin-Yuan (2014) "Synthesis, structural and optical properties of Sm³⁺ and Nd³⁺ doped cadmium sulfide nanocrystals" ,2014, 52 128–133.
- [22]. Jie, J.S., Zhang, W.J., Jiang, Y., Meng, X.M., Li, Y. Q. and Lee, S.T. (2006) Photoconductive Characteristics of Single-Crystal CdS Nanoribbons.
- [23]. Bangaru. Ravi Kumar, Dr. Samir Ranjan Meher (2016) Cadmium Sulfide (CdS) Based Thin Films for Photo Sensing Application" (IOSR-JAP) 47-55.